

## Dynamic characterization of fine-grained soils for the seismic microzonation of Central Italy

A. Ciancimino & S. Foti

*Politecnico di Torino, Italy*

G. Lanzo

*Università degli Studi di Roma La Sapienza, Italy*

G.A. Alleanza & A. d'Onofrio

*Università degli Studi di Napoli Federico II, Italy*

S. Amoroso

*Istituto Nazionale di Geofisica e Vulcanologia, L'Aquila, Italy*

R. Bardotti & C. Madiati

*Università degli Studi di Firenze, Italy*

G. Biondi & E. Cascone

*Università degli Studi di Messina, Italy*

F. Castelli & V. Lentini

*Università degli Studi di Enna Kore, Italy*

A. Di Giulio

*Istituto di Geologia Ambientale e Geoingegneria, CNR, Roma, Italy*

G. Vessia

*Università degli Studi G. d'Annunzio, Chieti – Pescara, Italy*

**ABSTRACT:** An accurate measurement of dynamic soil properties is essential to predict the nonlinear soil behavior under seismic loading conditions. This paper presents a database of cyclic and dynamic laboratory tests carried out after the 2016-2017 Central Italy Earthquake sequence, as part of the seismic microzonation studies in the area. The database consists of experimental results obtained on 79 samples investigated by means of dynamic resonant column tests, cyclic torsional shear tests or cyclic double specimen direct simple shear tests. The dynamic soil behavior is analyzed with reference to the small-strain wave velocity and damping ratio and to the modulus reduction and damping ratio curves. Experimental data are compared with the most widely used predictive models to underline the peculiarities of the investigated soils. Finally, a predictive model is calibrated to capture the nonlinear behavior of typical fine-grained soils from Central Italy.

### 1 INTRODUCTION

The stress-strain behaviour of soils under dynamic loads is commonly characterized with reference to the small-strain shear modulus ( $G_0$ ) and damping ratio ( $D_0$ ), along with the modulus reduction and damping (MRD) curves. The MRD curves describe the normalized secant shear modulus ( $G/G_0$ ) and the damping ratio ( $D$ ) as functions of the cyclic shear strain amplitude ( $\gamma_c$ ). Although the

recommended practice is to investigate the dynamic soil properties by means of laboratory tests, when experimental data are not available the MRD curves are usually derived from empirical models calibrated on similar soils (e.g. Vucetic & Dobry 1991; Darendeli 2001).

The predictive relationships are developed to capture the MRD curves according to the key parameters affecting the nonlinear soil behaviour, namely: the plasticity index ( $PI$ ), the effective mean confining stress ( $\sigma'_m$ ), the loading frequency ( $f$ ), the number of loading cycles ( $N$ ), and the over-consolidation ratio ( $OCR$ ) (e.g. Kokusho et al. 1982; Vucetic & Dobry 1991; d'Onofrio et al. 1999; Darendeli 2001). However, the curves show considerable differences depending on the combination of the adopted predictor variables (e.g. Kishida 2016). Specific relationships should then be adopted when site-specific response analyses are to be performed.

In this paper, the peculiarities of some fine-grained soils from Central Italy are analyzed with reference to a database of 79 dynamic and cyclic laboratory test results carried out on silts and clays. The database was developed within the context of the seismic microzonation studies of the municipalities most seriously damaged by the 2016-2017 Central Italy earthquake sequence. The sample disturbance effects are firstly analyzed by comparing the field and laboratory values of small-strain shear wave velocity ( $V_S$ ). Then, a comparative study between three families of MRD curves (i.e. Vucetic & Dobry 1991, Darendeli 2001, and Vardanega & Bolton 2013) and the experimental data is developed to highlight the specificities of the investigated soils.

Finally, the database is used to calibrate a specialized version of the widely adopted Darendeli (2001) model to capture the typical MRD curves of the tested soils from Central Italy.

## 2 DATABASE

In 2016-2017 a series of moderate to large earthquakes struck Central Italy, resulting in 298 casualties and more than 20,000 homeless, and almost completely destroying the historical villages of Amatrice, Accumoli and Arquata del Tronto. The seismic sequence started with an  $M_w$  6.0 mainshock on the 24<sup>th</sup> August 2016, which was followed by an  $M_w$  5.9 mainshock on 26<sup>th</sup> October 2016 to culminate on the 30<sup>th</sup> October 2016 with the largest shock of the sequence ( $M_w$  6.5). Other events occurred in the southern sector of the sequence on 18<sup>th</sup> January 2017, with a maximum  $M_w$  of 5.5 (Chiaraluce et al. 2017).

This sequence left behind a widespread damage across 138 municipalities distributed over four regions of Central Italy. Therefore, soon after the emergency, the Italian Government Commissioner for the Reconstruction sponsored and funded an ambitious project devoted to the seismic microzonation of these 138 municipalities, divided into 6 territorial units for organizational issues, namely: Abruzzo, Lazio, Umbria, Marche 1, Marche 2, and Marche 3 (Figure 1).

The project involved local authorities, researchers and consultants. It was coordinated by the *Center for Seismic Microzonation and its applications* (CentroMS, <https://www.centromicrozonazioneismica.it/en/>), an association of 25 research institutions and university departments providing expertise in a wide spectrum of disciplines: applied geophysics, engineering

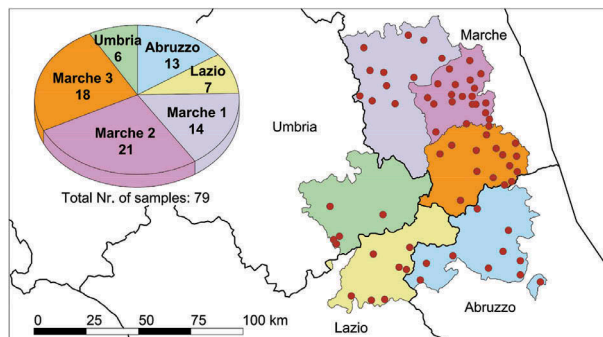


Figure 1. Locations of the 70 investigated sites in Central Italy and territorial distribution of the samples.

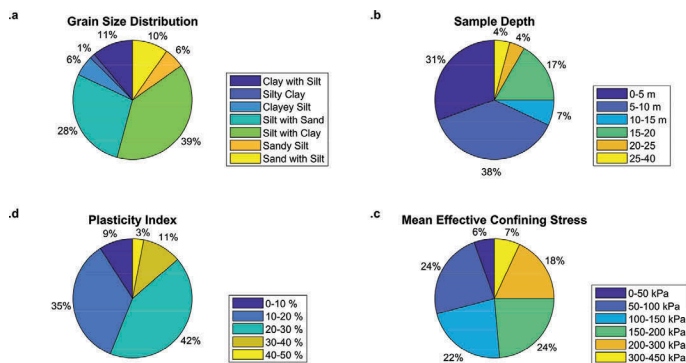


Figure 2. Characteristics of the samples: .a grain size distribution, .b sample depth, .c  $PI$ , and .d  $\sigma'_m$ .

seismology, geotechnical earthquake engineering and geology. Within this framework, several cyclic and dynamic tests were carried out to investigate the dynamic properties of soils in Central Italy. A database of experimental data was then compiled on the basis of the results of laboratory tests performed on samples from 70 municipalities. The locations of the investigated sites along with the geographical distribution of the samples are presented in Figure 1.

The compiled database includes both the index properties and the dynamic properties of the samples. The latter were obtained by dynamic resonant column (RC) tests, cyclic torsional shear (TS) tests or cyclic double specimen direct simple shear (DSDSS) tests. Measurements of the *in-situ*  $V_S$  were also included, taking advantages of the down-hole tests carried out in the same boreholes from which samples were retrieved. In total, the database holds information on 79 tests, namely: 9 RC tests, 51 combined RC/TS tests, and 19 DSDSS tests. However, TS tests were used mainly for comparisons with RC tests and therefore are not presented in this paper. Moreover, 7 RC tests were excluded from the following elaborations because resulted to be heavily affected by sample disturbance effects. In conclusion, the database subset here analyzed consists of 53 RC tests and 19 DSDSS tests. Further details can be found in Ciancimino et al. (in press).

The investigated soils consist mainly of silts with sand and clay, sampled up to a depth of 40 m. The soils are classifiable as low and normal active clays and silts of low plasticity with  $PI$  ranging from 0 to 45 %. Most of the specimens were tested at  $\sigma'_m$  comparable with the stress state expected on site, although some discrepancies were observed for a small number of tests. Distributions of the samples with respect to grain size distribution, sample depth,  $PI$ , and  $\sigma'_m$  are presented in the pie charts of Figure 2.

### 3 ANALYSIS OF RESULTS

The results of RC and DSDSS tests are presented in Figure 3 in terms of normalized shear modulus and damping ratio and, when available, pore-water pressure build-up ( $\Delta u$ ) versus  $\gamma_c$ . In this regard, only the RC devices were instrumented for pore water pressure measurements. Moreover, data are available only for 29 RC tests of the analyzed subset. The obtained scattering of experimental results reflects the wide range of  $PI$ ,  $\sigma'_m$  and  $f$  investigated by the cyclic tests. Specifically, a clear trend can be recognized between the  $G/G_0$  curves and  $PI$ , while the same trend is less marked for the  $D$  curves, probably due to the influence of the loading frequency on  $D_0$ .

#### 3.1 Small-strain shear wave velocity

The effect of the sample disturbance is analyzed with reference to the small-strain  $V_S$  obtained in laboratory ( $V_{S, lab}$ ) from the  $G_0$  values. Results are compared in Figure 4 with the values measured in field ( $V_{S, field}$ ) by means of down-hole tests. Experimental data are plotted according to the ratio  $A = \sigma'_m / z$  between the mean confining pressure applied in the laboratory tests and the depth of sampling. The  $A$  ratio is indicative of different reconsolidation processes: excessively

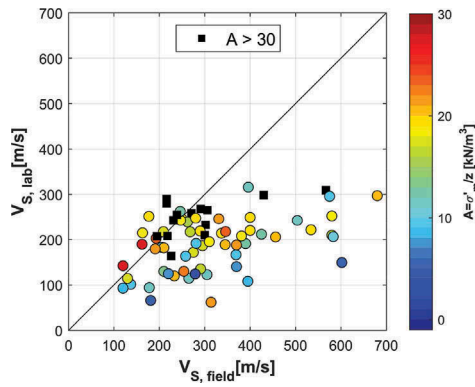


Figure 3. Results of 72 RC and DSDSS tests: a)  $G/G_0$  and  $D$ ; b) pore pressure build-up for 29 RC tests.

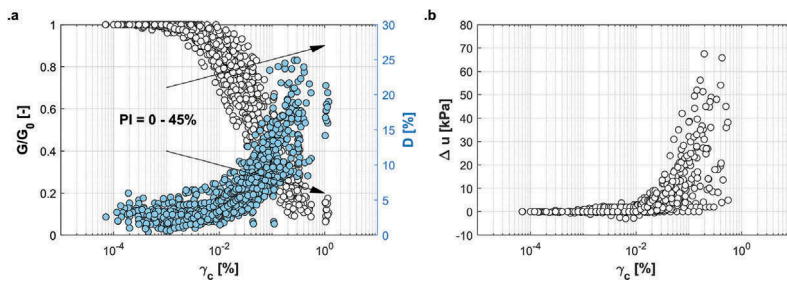


Figure 4. Comparison between laboratory and field values of small-strain shear wave velocity.

high  $A$  values ( $>22$ ) indicate that the specimens were reconsolidated at  $\sigma'_m$  higher than the confining *in situ* pressures, while specimens characterized by low  $A$  values ( $<10$ ) probably were not sufficiently reconsolidated. The testing  $\sigma'_m$  values were generally defined based on the expected *in situ* field values, except for some cases for which no information was available before the tests.

A marked reduction of the soil stiffness is observed for most of the samples. The sample disturbance affects mostly the hard soils (high  $V_{S, field}$ ) in agreement with the findings from the previous studies (Stokoe & Santamarina 2000). The reconsolidation process seems to play a role, although the trend is not very clear. On one hand, highly deformable soils reconsolidated at excessive  $\sigma'_m$  exhibit  $V_{S, lab}$  higher than the average range, with maximum values of about 1.4 times the  $V_{S, field}$ . On the other hand, reconsolidation processes carried out at  $\sigma'_m$  lower than the confining *in situ* pressure induce lower  $V_{S, lab}/V_{S, field}$  ratio, with minimum values of about 0.25.

### 3.2 Normalized shear modulus

Experimental results are compared in this section with the predictions of the models proposed by Vucetic & Dobry (1991), Darendeli (2001), and Vardanega & Bolton (2013).

Figure 5 plots  $\gamma_c$  against  $PI$  at four fixed  $G/G_0$  values (i.e. 0.99, 0.75, 0.5, and 0.25), in analogy with the plots presented by Kokusho et al. (1982) and Kishida (2016). The Darendeli (2001) relationships were implemented with reference to a constant mean  $\sigma'_m$  of 250 kPa and to an  $OCR$  of 1. The  $\gamma_c$  value that produces  $G/G_0$  of 0.99 is commonly identified to be the linear threshold shear strain (Vucetic 1994).

As expected, the experimental data show a growing trend of  $\gamma_c$  with  $PI$ , according to the predictive relationships plotted as reference. The linear threshold shear strain seems to be well captured only by the Vucetic & Dobry (1991) relationships, while the Darendeli (2001) and the Vardanega & Bolton (2013) models underestimate  $\gamma_{G/G_0=0.99}$ . Moreover, at small strains, a wide scatter of the data points is observed. At medium strain, all three predictive models show a good

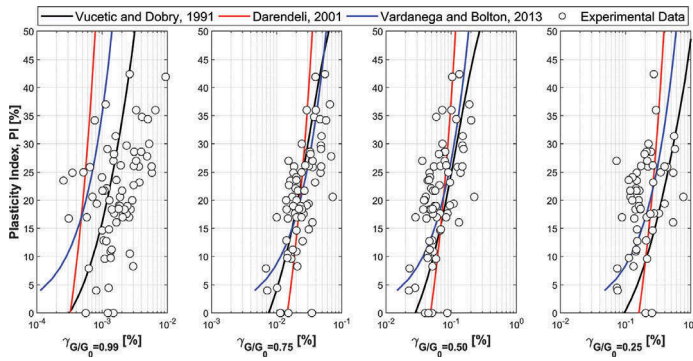


Figure 5. Variation of  $\gamma_c$  vs  $PI$  for fixed  $G/G_0$  values: 0.99, 0.75, 0.5, and 0.25.

fitting to the experimental data. On the contrary, the high strain range is well predicted by the Vardanega & Bolton (2013) model. Lastly, regarding this latter, it should be noted that it tends to underestimate the data when  $PI$  is less than 10 and it cannot be used for non-plastic soils.

### 3.3 Damping ratio

The analysis of the experimental data was performed considering separately  $D_0$  and the hysteretic  $D$  (i.e. the total  $D$  reduced by  $D_0$ ). As for the latter, Figure 6 reports the experimental data in terms of correlation between  $D - D_0$  and  $PI$  for three  $\gamma_c$  amplitudes (i.e. 0.01%, 0.1%, and 1%). The corresponding reference curves predicted by the Vucetic & Dobry (1991) and the Darendeli (2001) models are also represented. While the Darendeli (2001) model explicitly separates the contribute of  $D_0$  from the total  $D$ , the Vucetic & Dobry (1991) charts predict the total  $D$  values against  $\gamma_c$ . As a consequence, for consistency with the experimental data, the Vucetic & Dobry (1991) curves were reduced by a constant  $D_0$  of 1%, as predicted by the model in the small-strain range. The hysteretic  $D$  decreases with  $PI$  for all the strain levels considered. Both the predictive relationships are in good agreement with experimental data at medium strains (0.1%). At large strains (1%) the agreement with the two models is satisfactory, even if based on a few data, while the small-strain range is not well-captured. In particular, the Darendeli (2001) curve slightly overestimates the hysteretic  $D$ , reflecting the failure of the model in capturing the cyclic linear threshold. The Vucetic & Dobry (1991) curve is instead well above the experimental data range, probably due to the excessively low  $D_0$  value predicted to which the  $D$  curves are referred.

The measured  $D_0$  values are compared in Figure 7 with the predictions given by Darendeli (2001) depending on  $PI$ ,  $\sigma'_{mv}$ ,  $f$  (set equal to the laboratory values), and  $OCR$  (assumed to be 1). In the plot is also reported the range of  $D_0$  (i.e. 0.5-5.5%) identified by Vucetic & Dobry (1991), in which all the experimental data (except one) fall. The large data scattering confirms the

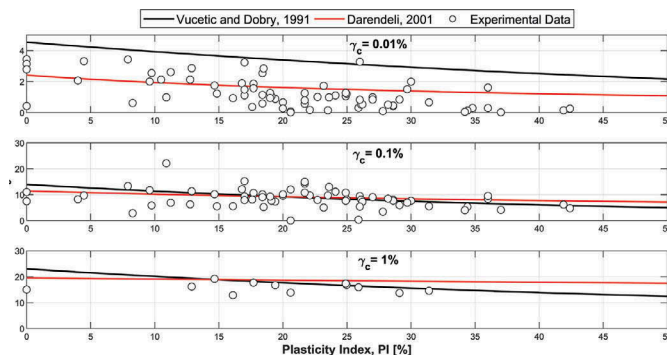


Figure 6. Variation of  $D$  vs  $PI$  for fixed  $\gamma_c$  values: 0.01%, 0.1%, and 1%.

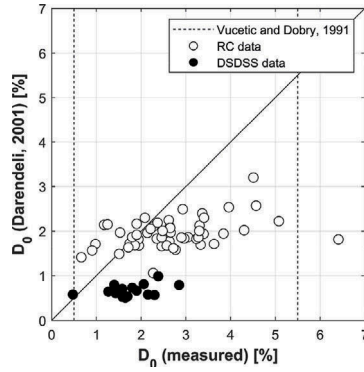


Figure 7. Measured vs predicted  $D_0$  values with reference to the Darendeli (2001) model; the dotted lines represent the range of  $D_0$  identified by Vucetic & Dobry (1991).

difficulties in the prediction of  $D_0$ . The Darendeli (2001) model seems to underestimate  $D_0$ , especially for DSDSS results. The differences between results from RC and DSDSS tests are probably due to the effect of  $f$  on  $D_0$ , which is not well captured by the predictive relationship.

#### 4 PREDICTIVE MODEL

An adjusted version of the predictive model proposed by Darendeli (2001) was calibrated to capture the MRD curves for Central Italy soils.

For the sake of simplicity, the influence of  $OCR$  and  $N$  was neglected in this study. The  $D_0$  is modelled taking into account separately the influence of  $PI$ ,  $\sigma'_m$ , and  $f$  through the following relationship (modified from Darendeli 2001):

$$D_0 = (\varphi_1 + \varphi_2 \cdot PI) \cdot \sigma'_m{}^{\varphi_3} \cdot [1 + \varphi_4 \cdot \ln(f)] \quad (1)$$

where  $PI$  is expressed in percentage,  $\sigma'_m$  in atm, and  $f$  in Hz.

The  $G/G_0$  curve is described through a modified version of the hyperbolic model proposed by Stokoe et al. (1999):

$$G/G_0 = \frac{1}{1 + \left(\frac{\gamma}{\gamma_r}\right)^a} \quad (2)$$

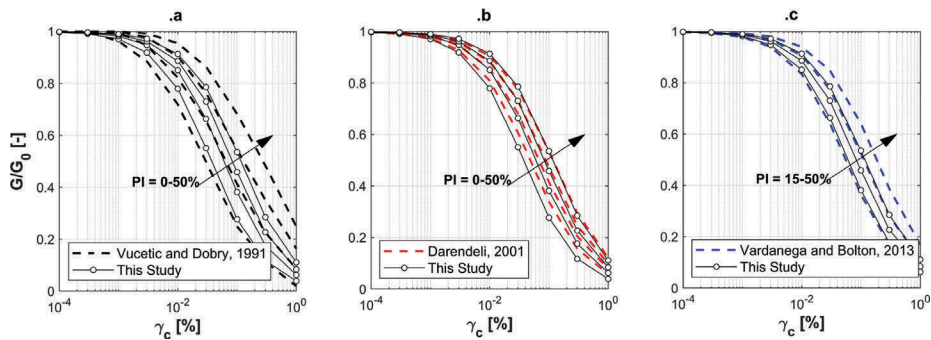


Figure 8. Comparison between predicted  $G/G_0$  curves with curves by a) Vucetic & Dobry (1991), b) Darendeli (2001), and c) Vardanega & Bolton (2013) for:  $PI = 0 - 50\%$ ;  $\sigma'_m = 250$  kPa;  $OCR = 1$ .

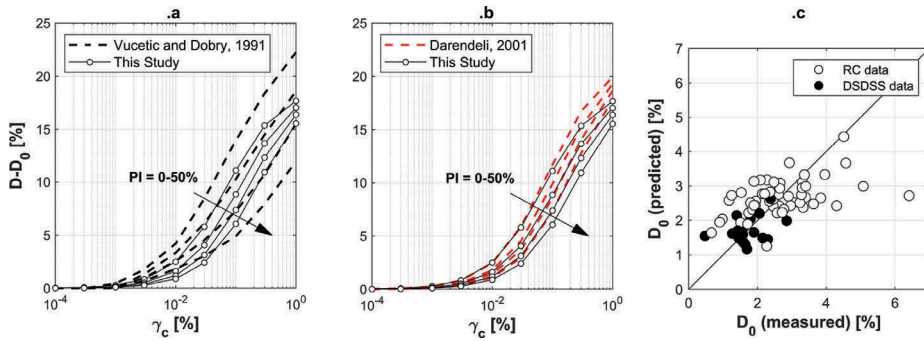


Figure 9. Comparison between: predicted  $D$  curves with curves by a) Vucetic & Dobry (1991) and b) Darendeli (2001) for:  $PI = 0\% - 50\%$ ;  $\sigma'_m = 250$  kPa;  $OCR = 1$ ; c) measured vs predicted  $D_0$  values.

Table 1. Model parameters obtained from the calibration

Parameter	$\varphi_1$	$\varphi_2$	$\varphi_3$	$\varphi_4$	$\varphi_5$	$\varphi_6$	$\varphi_7$	$\varphi_8$	$\varphi_9$
Mean value	1.281	0.036	-0.274	0.134	0.964	0.033	0.0014	0.125	0.506

where  $a = \varphi_5$  is the curvature parameter and  $\gamma_r$  is the reference strain which can be evaluated as follows (modified from Darendeli 2001):

$$\gamma_r = (\varphi_6 + \varphi_7 \cdot PI) \cdot \sigma'_m{}^{\varphi_8} \quad (3)$$

Following the procedure suggested by Darendeli (2001), the hysteretic  $D$  is modelled assuming the Masing (1926) criteria and fitting the experimental data by means of an adjusting function. The  $D$  curve is then given by the sum of  $D_0$  and the hysteretic  $D$  (Darendeli 2001):

$$D = \varphi_9 \cdot (G/G_0)^{0.1} \cdot D_{m \sin g} + D_0 \quad (4)$$

where  $D_{m \sin g}$  can be evaluated as a function of the  $G/G_0$  curve as suggested by Darendeli (2001).

The calibration of the model parameters (from  $\varphi_1$  to  $\varphi_9$ ) was performed applying a two-step procedure aiming at minimizing simultaneously the total error between the target and the model MRD curves. The results of the calibration are reported in Table 1. Further details about the procedure and the associated uncertainties can be found in Ciancimino et al. (in press).

Comparisons between the model calibrated in this study and the models proposed by Vucetic & Dobry (1991), Darendeli (2001), and Vardanega & Bolton (2013) are reported in Figures 8 and 9 in terms of MRD curves with reference to a  $\sigma'_m$  of 250 kPa, an  $OCR$  of 1 (adopted for the Darendeli 2001, curves), and with  $PI$  ranging from 0 % to 50 %. The MRD curves are less influenced by  $PI$  compared to the predictive models proposed by Vucetic & Dobry (1991) and Vardanega & Bolton (2013). A possible explanation is that the two literature models are not able to capture the influence of  $\sigma'_m$  and, in turn, part of the variability relating to  $\sigma'_m$  is associated with  $PI$ . However, it should be noted that although comparisons are not presented here, the effect of  $\sigma'_m$  on the MRD curves is not as significant as previously thought (Ciancimino et al. in press).

On the contrary, the predicted range is slightly broader than the one identified by Darendeli (2001). The two models are, anyway, similar and the updated model may not be able to properly capture the linear threshold. This is probably due to the modified hyperbolic relationship commonly used to describe the  $G/G_0$ , in conjunction with the Masing (1926) rules.

Figure 9c shows the comparison between predicted (Equation 1) and measured  $D_0$  values. Although a moderate scattering is still visible, the predictive relationship captures satisfactorily the experimental results. Specifically, the predicted values of  $D_0$  appears to be 0.5-1% higher than the  $D_0$  predicted by Darendeli (2001).

## 5 CONCLUSIONS

In this study, a database of 72 cyclic tests carried out on silty and clayey soils from Central Italy is analyzed with the aim of showing the distinctive features of the investigated soils.

Firstly, the effect of sample disturbance is investigated comparing the small-strain  $V_S$  values obtained by means of laboratory tests with the corresponding values measured in field. Soils characterized by higher  $V_{S, field}$  are more affected by the disturbance effect, exhibiting minimum  $V_{S, lab}/V_{S, field}$  ratios of about 0.25. Moreover, in a few cases of soft soils, the reconsolidation process may have played a role inducing an overestimation of  $V_{S, lab}$ .

The experimental results in terms of  $G/G_0$  and  $D$  versus  $\gamma_c$  are then compared to the models proposed by Vucetic & Dobry (1991), Darendeli (2001), and Vardanega & Bolton (2013). For the  $G/G_0$  curves, the models are able to capture the soil nonlinearity at intermediate strain levels, while some discrepancies are observed at small and large strains. In particular, both the Darendeli (2001) and the Vardanega & Bolton (2013) models fail to capture the experimental cyclic linear thresholds. For the Darendeli (2001) model, this is reflected also in the  $D$  ratio curves with an overestimation of the hysteretic  $D$  at small strains. The Vucetic & Dobry (1991) curves are instead in good agreement with experimental data in terms cyclic linear thresholds, while a marked overestimation of the hysteretic  $D$  is observed at small strains, probably due to the low  $D_0$  to which the  $D$  curves are referred.  $D_0$  experimental values are characterized by large scattering. Moreover, the comparison between the experimental values and the estimates given by the Darendeli (2001) relationship revealed an underestimation of  $D_0$ .

Finally, a predictive model is calibrated on the basis of the framework defined by Darendeli (2001). The model can capture the dynamic properties of the tested fine-grained soils in terms of MRD curves and  $D_0$ . However, the experimental linear thresholds are not totally captured, probably because of the modified hyperbolic relationship adopted to predict the  $G/G_0$  curves.

## REFERENCES

- Chiaraluce, L., Di Stefano, R., Tinti, E., Scognamiglio, L., Michele, M., Casarotti, E., Cattaneo, M., De Gori, P., Chiarabba, C., Monachesi, G., Lombardi, A., Valoroso, L., Latorre, D. & Marzorati, S. 2017. The 2016 central Italy seismic sequence: A first look at the mainshocks, aftershocks, and source models. *Seismological Research Letters*, 88, 757-771.
- Ciancimino, A., Lanzo, G., Alleanza, G. A., Amoroso, S., Bardotti, R., Biondi, G., Cascone, E., Castelli, F., Di Giulio, A., D'Onofrio, A., Foti, S., Lentini, V., Madiati, C. & Vessia, G. in press. Dynamic characterization of fine-grained soils in Central Italy by laboratory testing. *Bulletin of Earthquake Engineering*.
- D'Onofrio, A., Silvestri, F. & Vinale, F. 1999. Strain rate dependent behaviour of a natural stiff clay. *Soils and Foundations*, 39, 69-82.
- Darendeli, M. B. 2001. *Development of a new family of normalized modulus reduction and material damping curves*. PhD Dissertation, University of Texas at Austin.
- Kishida, T. 2016. Comparison and correction of modulus reduction models for clays and silts. *Journal of Geotechnical and Geoenvironmental Engineering*, 143, 04016110.
- Kokusho, T., Yoshida, Y. & Esashi, Y. 1982. Dynamic properties of soft clay for wide strain range. *Soils and Foundations*, 22, 1-18.
- Masing, G. Eigenspannumyen und verfeshungung beim messing. Proc. Inter. Congress for Applied Mechanics, 1926. 332-335.
- Stokoe, K., Darendeli, M., Andrus, R. & Brown, L. Dynamic soil properties: laboratory, field and correlation studies. Proc. 2nd Int. Conf. Earthquake Geotech. Engg. 1999. 811-846.
- Stokoe, K. & Santamarina, J. C. Seismic-wave-based testing in geotechnical engineering. ISRM International Symposium, 2000. International Society for Rock Mechanics.
- Vardanega, P. & Bolton, M. 2013. Stiffness of clays and silts: Normalizing shear modulus and shear strain. *Journal of Geotechnical and Geoenvironmental Engineering*, 139, 1575-1589.
- Vucetic, M. 1994. Cyclic threshold shear strains in soils. *Journal of Geotechnical engineering*, 120, 2208-2228.
- Vucetic, M. & Dobry, R. 1991. Effect of soil plasticity on cyclic response. *Journal of geotechnical engineering*, 117, 89-107